AIP ADVANCES **5**, 057106 (2015)

Spatial and spectral distributions of thermal radiation emitted by a semi-infinite body and absorbed by a flat film

Etienne Blandre,[1,a] Pierre-Olivier Chapuis,[1] Mathieu Francoeur,[2] and Rodolphe Vaillon[1]
[1]*Université de Lyon, CNRS, INSA-Lyon, UCBL, CETHIL, UMR5008, F-69621, Villeurbanne, France*
[2]*Department of Mechanical Engineering, University of Utah, Salt Lake City, UT 84112, USA*

(Received 5 March 2015; accepted 15 April 2015; published online 5 May 2015)

We analyze the radiative power emitted by a semi-infinite medium and absorbed by a flat film located in its vicinity. In the near-field regime, if the film is thin enough, the surface waves at the rear interface of the film can contribute to the heat transfer. As a result, the absorbed power can be enhanced farther from the front surface. In the near-to-far field transition regime, temporal coherence of thermal radiation and the associated interferences can be used to shape the spectrum of the transferred radiative heat flux by selecting approriate geometrical parameters. These results highlight possibilities to control both the location where the radiative power is absorbed in the film and the spectral distribution, which are of paramount importance for applications such as near-field thermophotovoltaics. [http://dx.doi.org/10.1063/1.4919931]

I. INTRODUCTION

Because Planck's blackbody spectral distribution of thermal radiation does not take the contribution of evanescent waves into account, it is not valid anymore in the near-field, where radiative transfer via tunneling of evanescent waves is dominant. In the case of two planar parallel bodies separated by a subwavelength distance, this leads to a large increase of the radiative heat flux[1,2] and, in the particular case of materials supporting surface phonon-polaritons (SPhPs) or surface plasmon-polaritons (SPPs), to the apparition of resonances in the spectrum of thermal radiation.[3] The first clear experimental evidences of these near-field enhancements were for tip-plane[4] and sphere-plane[5–8] configurations. Even the modification of the radiative spectrum[9–11] could be measured recently. The plate-plate configuration, which is the most relevant for applications, was investigated experimentally as well and could confirm the theoretical predictions.[12–15] One of the promising applications is thermophotovoltaic power generation with near-field radiation enhancement.[16,17] The principle is to harvest waste energy from a thermally-radiating emitter brought in the vicinity of a low bandgap photovoltaic cell. Understanding how the radiated power is absorbed within the cell, where the electrical charges are generated, is of paramount importance. Prior to analyzing this specific issue, the physics of thermal radiation between a semi-infinite plane emitter and a film or a film on a substrate must be clarified. Previous modeling works investigated metallic[18] and dielectric[19] coatings on substrates. It was shown that the coupling of SPhPS or SPPs in the coating can improve heat transfer. Near-field radiative heat transfer between thin films was analyzed by Refs. 20 and 21, where it was shown in particular that the film sizes can impact the spectral shape at the resonances. Concerning the spatial absorption of near-field radiative power, a previous work[22] showed that because of their large momentum, evanescent modes have a very low penetration depth, that has been evaluated as approximately $0.2d$ in the case of two parallel plates separated by a

[a]Electronic mail: etienne.blandre@insa-lyon.fr

vacuum gap of size d. Another group[23,24] studied the variation of the penetration depth inside hyperbolic metamaterials, where the impact of frustrated modes on the spatial absorption is significant. Indeed, these modes are propagative inside the absorber, so they are expected to have a larger penetration depth than surface modes. Finally, it was observed for the case of two semi-infinite media that another regime can appear when the distance separating the bodies is close to the value of the characteristic wavelength of thermal radiation. At such distances, evanescent waves can still be negligible while temporal coherence effects of thermal radiation due to interferences of propagative waves lead to a modification of the power exchanged by the two bodies.[25,26]

Here we focus on the configuration involving radiative heat transfer from a semi-infinite emitter towards a flat film, from the near-field to the far-field regimes and we study the spatial distribution of the radiation absorbed inside the film. We specifically investigate the transition between the near-field and the far-field regimes, observing how interferences can affect the spectrum of thermal radiation and the total radiative power transferred from the semi-infinite emitter to the film.

II. STUDIED CONFIGURATION AND METHOD

The configuration is the following: medium 1, a semi-infinite emitter, is separated by a vacuum gap (medium 2) of size d from medium 3, a film of finite thickness t. Medium 4 at the rear of the film is vacuum. The emitter and the film are made of the same material. Two typical materials are studied: one with a spectral resonance, silicon carbide (SiC), with a dielectric function modelled by a damped oscillator (Lorentz model),[21] and a material modelled by a non-resonant dielectric function taken as $\epsilon = 20 + 0.01i$. The temperature of the emitter is denoted T_{emit}, and as we are only interested in the radiative power emitted by medium 1 and absorbed by medium 3, the latter is assumed to be non-emitting ($T_{film} = 0$ K).

To derive the radiative heat flux, we use fluctuationnal electrodynamics:[27] Maxwell's equations are solved using dyadic Green's functions, which link the electromagnetic excitation of a medium with the response of another medium, and the Fluctuation-Dissipation Theorem, that provides the stochastic charge density due to thermal motion. To analyze the spatial distribution of thermal radiation absorbed inside the film, it is divided into control volumes. The required Green's functions at each depths z are computed numerically with a scattering matrix approach.[28] Radiation absorbed in each control volume is then given by the difference between the radiative heat fluxes q at the boundaries of the control volume. The absorbed power per unit volume at each depth z is given by the radiated power absorbed by a control volume, divided by its size. The propagative and evanescent components of the monochromatic radiative heat flux at the entrance of the film can also be derived analytically, and their expressions are given by:[21]

$$q_\omega^{prop}(z=0) = \frac{\Theta(\omega, T_{emit})}{4\pi^2} \int_0^{\frac{\omega}{c}} k_\rho dk_\rho \underbrace{\sum_{\gamma=s,p} \frac{(1-|r_{21}^\gamma|^2)(1-|R_3^\gamma|^2)}{|1-r_{21}^\gamma R_3^\gamma e^{2ik_{z_2}d}|^2}}_{T_e^\gamma(k_\rho \le \frac{\omega}{c}, \omega)} \tag{1}$$

$$q_\omega^{evan}(z=0) = \frac{\Theta(\omega, T_{emit})}{\pi^2} \int_{\frac{\omega}{c}}^{\infty} k_\rho dk_\rho \underbrace{e^{-2\mathrm{Im}(k_{z_2})d} \sum_{\gamma=s,p} \frac{\mathrm{Im}(r_{21}^\gamma)\mathrm{Im}(R_3^\gamma)}{|1-r_{21}^\gamma R_3^\gamma e^{2ik_{z_2}d}|^2}}_{T_e^\gamma(k_\rho > \frac{\omega}{c}, \omega)} \tag{2}$$

where ω is the angular frequency, c is the speed of light in vacuum, $\Theta(\omega, T_{emit})$ is the mean energy of a Planck oscillator, r_{21}^γ is the Fresnel's reflection coefficient at the interface 21 where γ stands for the s or p-polarizations, and R_3^γ is the reflection coefficient of the film, whose expression is given by:

$$R_3^\gamma = \frac{r_{12}^\gamma + r_{23}^\gamma e^{2ik_{z_3}t}}{1 + r_{12}^\gamma r_{23}^\gamma e^{2ik_{z_3}t}}. \tag{3}$$

k_z and k_ρ denote the components of the wavevector respectively perpendicular and parallel to the interface. The factors above the braces correspond to the so-called transmission factor T_e^γ. The total heat flux is the integral over frequencies of the summation of the propagative and evanescent components. To analyze the contributions of the wave modes in the various parts of the system, the radiative heat flux is divided into three components:

- for $0 \leq k_\rho < \frac{\omega}{c}$, the waves are propagative in the emitter, the vacuum gap and the film. They are termed fully-propagative modes.
- for $\frac{\omega}{c} \leq k_\rho < \frac{\omega n}{c}$, where n is the real part of the complex refractive index of the material, the waves are propagative in the emitter, evanescent in the vacuum gap as a result of total internal reflection, and propagative in the film.[29] They are called frustrated or mixed propagative–evanescent modes.
- for $\frac{\omega n}{c} \leq k_\rho < \infty$, the waves are evanescent in the emitter, the vacuum gap and the film. These are the fully-evanescent or surface modes.

III. ENHANCEMENT OF NEAR-FIELD ABSORPTION DUE TO THE EXCITATION OF SURFACE WAVES AWAY FROM THE SURFACE CLOSE TO THE EMITTER

We first analyze the radiative heat transfer in the near-field regime in the case of SiC, which is a polar material that supports SPhPs in the infrared. It is known that the surface waves of two identical interfaces can couple inside a cavity. If the two branches of the dispersion relation of the SPhPs overlap, they split into symmetric and antisymmetric modes.[3] Figure 1 depicts the p-polarized transmission coefficient T_e^p in the (k_ρ,ω) plane, for a distance d = 100 nm and two thicknesses t. When the film is thick (t = 10 μm, 1.a), the two branches of the SPhPs dispersion relation are equivalent to the case of two semi-infinite media separated by a vacuum gap size d = 100 nm. When the film is thin enough (t = 100 nm, Fig. 1(b)), the surface wave at the opposite side of the film can be excited, leading to the apparition of a third resonance branch. The upper and lower branches are the result of the coupling of the SPhPs of two interfaces of the system, that overlap and split into symmetric and antisymmetric modes.[30] The middle branch comes from the last interface, and as it cannot overlap with another one, its equation is the same as the case of a single SiC-vacuum interface. In the supplemental material,[31] we clearly show that the absorption is due to hybridized surface modes in the vacuum gap. The excited mode at the rear interface is a single interface mode.

Next, we analyze in details the spatial distribution of the absorbed near-field thermal radiation inside the thin film. The temperature of the emitter is set at T_{emit} = 800 K. In Fig. 1(c), we report the radiative power absorbed per unit volume as a function of depth for d = 100 nm and t = 100 nm. The evanescent waves have a low penetration depth, such that the absorption inside a thin film is dominated by the fully evanescent component. The absorbed power is exponentially decreasing when the depth increases, but it raises again next to the back interface of the film, because of the excitation of the surface wave at this interface. This underlines the possibility of increasing the absorption farther from the surface facing medium 1.

IV. IMPACT OF PROPAGATIVE, EVANESCENT AND FRUSTRATED MODES ON SPATIAL ABSORPTION IN THE NEAR-FIELD REGIME

Absorption by a thicker film (t = 10 μm) is now under consideration. In Fig. 2(a), the spatial absorption profile is plotted for a vacuum gap size d = 100 nm, and decomposed into the three types of modes. The sum of the three contributions exhibits two regions: on the first hundred nanometers, the absorption is dominated by the fully-evanescent component, that decays quickly due to the low penetration depth (of the order of magnitude of the vacuum gap d for materials supporting SPhPs). At larger depths, absorption is dominated by the frustrated modes, because of their larger penetration depths. In Fig. 2(b), the spectral distribution of the radiative power is depicted. We observe the impact of SPhPs around the resonance frequencies, between $\omega = 1.5 \times 10^{14}$ and $\omega = 1.9 \times 10^{14}$ rad.s^{-1}. They induce a high absorption on the first hundred nanometers. At larger distances, their role is negligible, and absorption is mostly due to the frustrated modes, that have

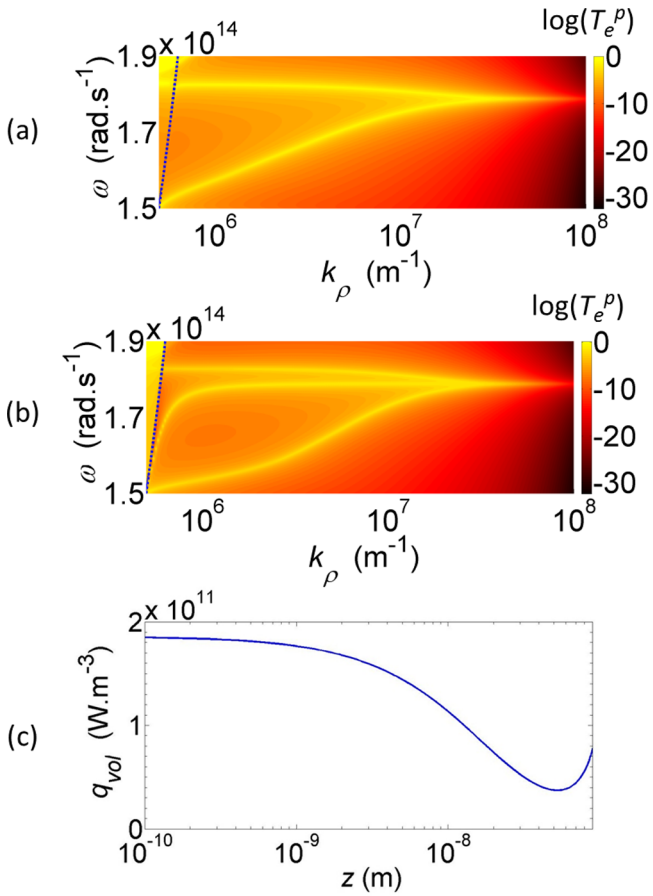

FIG. 1. p-polarized transmission coefficient T_e^p as a function of k_ρ and ω. (a) $d = 100$ nm and $t = 10$ μm (b) $d = 100$ nm and $t = 100$ nm (c) Radiative power absorbed per unit volume as a function of depth z, for a temperature $T_{emit} = 800$ K, $d = 100$ nm and $t = 100$ nm.

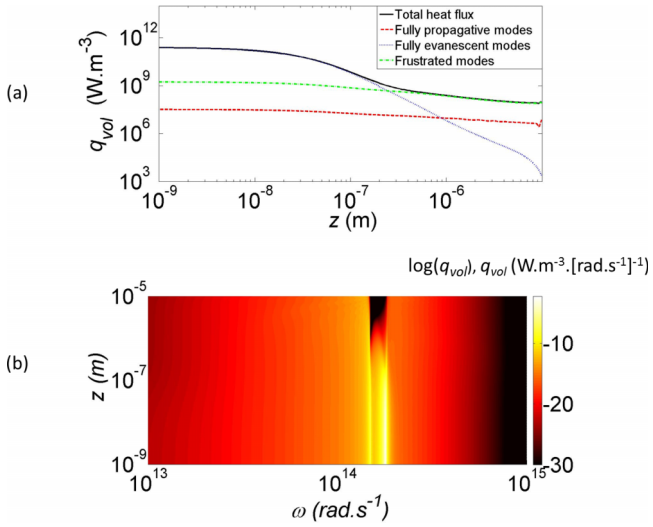

FIG. 2. (a) Radiative power absorbed per unit volume as a function of depth z. (b) Radiative power absorbed per unit volume as a function of depth z and angular frequency ω for $t = 10$ μm and $d = 100$ nm.

a high intensity for a frequency slightly lower than $\omega = 1.5 \times 10^{14}$ rad.s^{-1}, where the real part of the refractive index n is large. The previous results indicate that absorption in given frequency ranges happens preferentially at given depths. Thus it might be possible to chose which part of the spectrum should be absorbed at which location.

V. SPECTRAL CONTROL OF ABSORPTION USING INTERFERENCES IN THE NEAR-TO-FAR FIELD TRANSITION REGIME

The near-to-far field transition regime is analyzed next. This regime can be observed when the size of the cavity is similar to the characteristic wavelength of thermal radiation, approximately given by Wien's law. At this distance, propagative waves are reflected and can interfere, exhibiting effects of temporal coherence of thermal radiation. In Fig. 3, we plot the p-polarized transmission coefficient T_e^p in the case of a constant dielectric function $\epsilon = 20 + 0.01i$. The emitter is at $T_{emit} = 300$ K, and the corresponding characteristic wavelength of thermal radiation is close to 10 μm. The (k_ρ,ω) plots are decomposed into three areas: the blue dashed line is the curve of equation $\omega = k_\rho c$, and all modes on the left of this curve are fully propagative; the green line is the curve of equation $\omega = \frac{k_\rho c}{n}$, and all modes on the right of this line are fully evanescent in the medium; the modes that are located between those two curves correspond to the propagative-evanescent or frustrated modes.

In the fully propagative area of the (k_ρ,ω) plots (Figs. 3(a) and 3(b)), we can see the apparition of fringes that are caused by interferences, and represent the resonant modes inside the cavity, similarly to.[25,26] In the second configuration (Fig. 3(b)), the thickness of the film is set at 10 μm as well as the size of medium 2 (vacuum gap). As the characteristic wavelength of thermal radiation inside the film $\frac{\lambda_0}{n}$ is close to the thickness of the film, interferences can also occur in the film. In the T_e^p representation, we observe the apparition of resonant modes due to interferences in the component related to the frustrated modes. We note that the quality factors associated to the resonances of the frustrated modes are much larger than the ones of the fully propagative modes. These results suggest that it might be possible to enhance the impact of interferences in the spectrum of the transferred power by choosing appropriate film thicknesses and vacuum gap sizes. For instance, Fig. S3 of the supplemental material[31] shows the impact of interferences in the film on the spatial and spectral distribution of the absorbed radiative power.

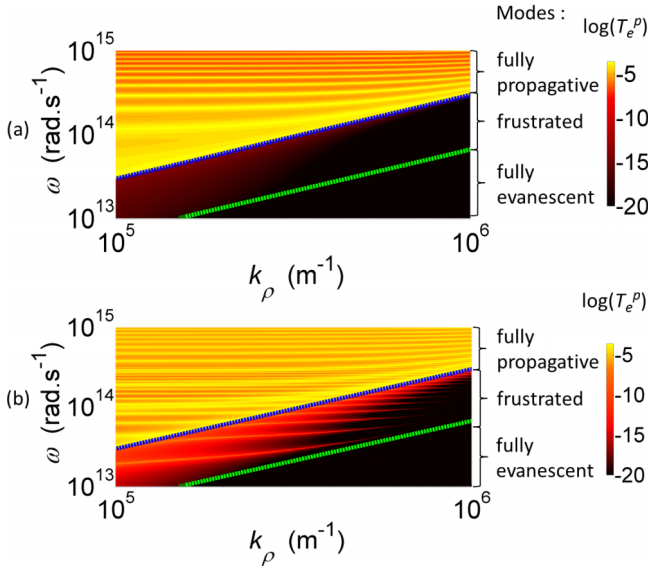

FIG. 3. p-polarized component of the transmission factor T_e^p for a constant dielectric function, as a function of k_ρ and ω. The colormap is in logarithmic scale. The blue dashed line represents the curve of equation $\omega = k_\rho c$ and the green dashed line represents the curve of equation $\omega = \frac{k_\rho c}{n}$. (a) $d = 10$ μm and $t = 100$ nm (b) $d = 10$ μm and $t = 10$ μm.

We underline that the same effects happen with realistic dielectric functions associated to metals and dielectrics (see the example of SiC in the supplemental material[31]). For instance, the real and imaginary parts of the dielectric function of SiC is almost constant outside the reststrahlen band for frequencies populated at usual temperatures, and the values are of the same order as that of our example. The analysis is just simplified in our case.

VI. SUMMARY AND PERSPECTIVES

We have shown that the spectral and spatial distributions of radiative heat flux emitted by a semi-infinite body and absorbed by a flat film can be tuned by adjusting the geometric parameters. The impact of surface waves on the spatial distribution has also been underlined. Specific values of the vacuum gap size and the film thickness can give rise to interferences that modify the heat flux absorbed by the film. All these effects suggest strategies to improve the selectivity of the absorption in terms of spatial or spectral location. Due to their low penetration depths, SPhPs induce a high generation of electrical charges close to the surface of the near-field thermophotovoltaic cells, and the charges are likely to recombine without generating electrical power thus leading to significant electrical losses.[32–34] The control of the absorption of near-field thermal radiation within the cell is a mean to solve this problem. As a consequence, this work highlights a way for improving the efficiency of near-field thermophotovoltaic devices.

E.B and P.O.C. acknowledge the partial support of project ANR 11-PDOC-0024 Nanoheat. M.F. acknowledges the financial support provided by the National Science Foundation under Grant No. CBET-1253577.

[1] D. Polder and M. Van Hove, "Theory of radiative heat transfer between closely spaced bodies," Physical Review B **4**, 3303–3314 (1971).
[2] M. Francoeur and M. Mengüç, "Role of fluctuational electrodynamics in near-field radiative heat transfer," Journal of Quantitative Spectroscopy and Radiative Transfer **109**, 280–293 (2008).
[3] K. Joulain, J.-P. Mulet, F. Marquier, R. Carminati, and J.-J. Greffet, "Surface electromagnetic waves thermally excited: Radiative heat transfer, coherence properties and casimir forces revisited in the near field," Surface Science Reports **57**, 59–112 (2005).
[4] A. Kittel, W. Müller-Hirsch, J. Parisi, S.-A. Biehs, D. Reddig, and M. Holthaus, "Near-field heat transfer in a scanning thermal microscope," Physical Review Letters **95**, 224301 (2005).
[5] S. Shen, A. Narayanaswamy, and G. Chen, "Surface phonon polaritons mediated energy transfer between nanoscale gaps," Nano Letters **9**, 2909–2913 (2009).
[6] E. Rousseau, A. Siria, G. Jourdan, S. Volz, F. Comin, J. Chevrier, and J.-J. Greffet, "Radiative heat transfer at the nanoscale," Nature Photonics (2009).
[7] S. Shen, A. Mavrokefalos, P. Sambegoro, and G. Chen, "Nanoscale thermal radiation between two gold surfaces," Applied Physics Letters **100**, 233114 (2012).
[8] B. Song, Y. Ganjeh, S. Sadat, D. Thompson, A. Fiorino, V. Fernández-Hurtado, J. Feist, F. J. Garcia-Vidal, J. C. Cuevas, P. Reddy, and E. Meyhofer, "Enhancement of near-field radiative heat transfer using polar dielectric thin films," Nature Nanotechnology (2015), 10.1038/nnano.2015.6.
[9] A. C. Jones and M. B. Raschke, "Thermal infrared near-field spectroscopy," Nano Letters **12**, 1475–1481 (2012).
[10] A. Babuty, K. Joulain, P.-O. Chapuis, J.-J. Greffet, and Y. De Wilde, "Blackbody spectrum revisited in the near field," Physical Review Letters **110**, 146103 (2013).
[11] B. T. O'Callahan, W. E. Lewis, A. C. Jones, and M. B. Raschke, "Spectral frustration and spatial coherence in thermal near-field spectroscopy," Physical Review B **89**, 245446 (2014).
[12] C. Hargreaves, "Anomalous radiative transfer between closely-spaced bodies," Physics Letters A **30**, 491–492 (1969).
[13] L. Hu, A. Narayanaswamy, X. Chen, and G. Chen, "Near-field thermal radiation between two closely spaced glass plates exceeding planck's blackbody radiation law," Applied Physics Letters **92**, 133106 (2008).
[14] T. Kralik, P. Hanzelka, M. Zobac, V. Musilova, T. Fort, and M. Horak, "Strong near-field enhancement of radiative heat transfer between metallic surfaces," Physical Review Letters **109**, 224302 (2012).
[15] R. S. Ottens, V. Quetschke, S. Wise, A. A. Alemi, R. Lundock, G. Mueller, D. H. Reitze, D. B. Tanner, and B. F. Whiting, "Near-field radiative heat transfer between macroscopic planar surfaces," Phys. Rev. Lett. **107**, 014301 (2011).
[16] M. Whale and E. G. Cravalho, "Modeling and performance of microscale thermophotovoltaic energy conversion devices," Energy Conversion, IEEE Transactions on **17**, 130–142 (2002).
[17] R. S. DiMatteo, P. Greiff, S. L. Finberg, K. A. Young-Waithe, H. K. H. Choy, M. M. Masaki, and C. G. Fonstad, "Enhanced photogeneration of carriers in a semiconductor via coupling across a nonisothermal nanoscale vacuum gap," Applied Physics Letters **79**, 1894–1896 (2001).
[18] S.-A. Biehs, "Thermal heat radiation, near-field energy density and near-field radiative heat transfer of coated materials," The European Physical Journal B **58**, 423–431 (2007).
[19] M. Francoeur, M. P. Mengüç, and R. Vaillon, "Near-field radiative heat transfer enhancement via surface phonon polaritons coupling in thin films," Applied Physics Letters **93**, 043109 (2008).

[20] P. Ben-Abdallah, K. Joulain, J. Drevillon, and G. Domingues, "Near-field heat transfer mediated by surface wave hybridization between two films," Journal of Applied Physics **106**, 044306 (2009).
[21] M. Francoeur, M. Mengüç, and R. Vaillon, "Spectral tuning of near-field radiative heat flux between two thin silicon carbide films," Journal of Physics D: Applied Physics **43**, 075501 (2010).
[22] S. Basu and Z. M. Zhang, "Ultrasmall penetration depth in nanoscale thermal radiation," Applied Physics Letters **95**, 133104 (2009).
[23] M. Tschikin, S.-A. Biehs, P. Ben-Abdallah, S. Lang, A. Petrov, and M. Eich, "Transport of radiative heat flux by hyperbolic metamaterials," ArXiv e-prints (2014).
[24] S. Lang, M. Tschikin, S.-A. Biehs, A.-Y. Petrov, and M. Eich, "Large penetration depth of near-field heat flux in hyperbolic media," Applied Physics Letters **104**, 121903 (2014).
[25] J. Mayo and A. Narayanaswamy, "Minimum radiative transfer between two metallic planar surfaces," in *Proceedings of the 11th AIAA/ASME Joint Thermophysics and Heat Transfer Conference*, *Atlanta, USA*, *June 16-20* (2014).
[26] Y. Tsurimaki, P.-O. Chapuis, R. Vaillon, J. Okajima, A. Komiya, and S. Murayama, "Reducing thermal radiation between parallel plates in the far-to-near field transition regime," in *Proceedings of the 15th International Heat Transfer Conference*, *Kyoto, Japan*, *Aug. 10-15* (2014).
[27] S. Rytov, I. Kravtsov, and V. Tatarskii, "Principles of Statistical Radiophysics: Elements of random fields," *Principles of Statistical Radiophysics* (Springer-Verlag, 1989).
[28] M. Francoeur, M. Mengüç, and R. Vaillon, "Solution of near-field thermal radiation in one-dimensional layered media using dyadic green's functions and the scattering matrix method," Journal of Quantitative Spectroscopy and Radiative Transfer **110**, 2002–2018 (2009).
[29] E. Rousseau, M. Laroche, and J.-J. Greffet, "Asymptotic expressions describing radiative heat transfer between polar materials from the far-field regime to the nanoscale regime," Journal of Applied Physics **111**, 014311 (2012).
[30] E. N. Economou, "Surface plasmons in thin films," Physical Review **182**, 539–554 (1969).
[31] See supplementary material at http://dx.doi.org/10.1063/1.4919931 for the analysis of the participating modes as a function of the depth in the layer.
[32] K. Park, S. Basu, W. King, and Z. Zhang, "Performance analysis of near-field thermophotovoltaic devices considering absorption distribution," Journal of Quantitative Spectroscopy and Radiative Transfer **109**, 305–316 (2008), the Fifth International Symposium on Radiative Transfer.
[33] M. Francoeur, R. Vaillon, and M. Mengüç, "Thermal impacts on the performance of nanoscale-gap thermophotovoltaic power generators," Energy Conversion, IEEE Transactions on **26**, 686–698 (2011).
[34] M. P. Bernardi, O. Dupré, E. Blandre, P.-O. Chapuis, R. Vaillon, and M. Francoeur, "Impacts of propagating, frustrated and surface modes on radiative, electrical and thermal losses in nanoscale-gap thermophotovoltaic power generators," arXiv e-prints (2015).